Case Studies in Construction Materials 17 (2022) e01235

Contents lists available at ScienceDirect

Case Studies in Construction Materials

journal homepage: www.elsevier.com/locate/cscm

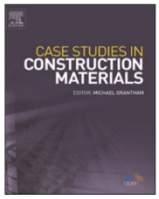

Case study

Numerical investigation of the seismic vulnerability of bridge piers strengthened with steel fibre reinforced concrete (SFRC) and carbon fibre composites (CFC)

S. Harzallah [a,*], M. Chabaat [a], M. Saidani [b], M. Moussaoui [a]

[a] 2,4 Built Environmental Research Lab., Dept. of Structures and Materials, Civil Engineering Faculty, University of Sciences and Technology Houari Boumediene, B.P. 32 El Alia Bab Ezzouar, 16111 Algiers, Algeria
[b] School of Energy, Construction and Environment, Coventry University, Priory Street, Coventry, UK

ARTICLE INFO

Keywords:
Dynamic analysis
Non-linear static analysis
Bridge piers
Dynamic finite element system
Composite material mixture
Reinforced concrete pier

ABSTRACT

This research proposes a method aimed at investigating the detection of bridge damage areas using a rigorous method based on mathematical models of dynamic finite elements. Strengthening of the reinforced concrete (RC) is proposed for increasing the strength of RC structures when they present material degradation. It includes reinforcement with carbon reinforcement composites (CFC) and steel fiber reinforced concrete (SFRC), injection with SikaDur 52 Injection type epoxy resin, and the addition of SikaTop 126 type concrete. Establishment of a set of equations and numerical modeling of the specified method are presented in this study for sparse matrices of a large system of equations. A numerical solver with FEM Ansys software was used to avoid the lack of big-data memory storage on the available hardware. RC material properties have been modeled with the composite material mixture laws as a homogeneous material. Several simulations have been achieved. The results obtained allowed location of stress concentration areas and consequently, detection of important von-Mises equivalent stresses of strength bound in severe load cases as well as graphically visualization of the time history of displacements evolution. The study has also revealed that the reliability design of the probabilistic method with the security margin as a stochastic variable is an effective structural health monitoring approach.

1. Introduction

Concrete structures can suffer damage for a number of reasons such as traffic evolution, road accidents, changes in climatic actions or loading in buildings [1,2]. To solve these problems, two principal solutions are proposed to the project owners: reconstruction or repair. Rebuilding is an interesting solution but it is very costly and cannot be used for all structures and in particular, historical structures. The second solution is often used to maintain the structures in a good serviceable condition [3].

The technique of external strengthening of RC structures is usually used in the rehabilitation or increase of resistance where there is material degradation, design error, or when the current loading requires a more resistant structure for safety [4]. Among the commonly used repair methods is the application of composite materials to the strengthening of RC structures [5]. The relatively acceptable costs

* Corresponding author.
E-mail addresses: harzallahozil@yahoo.fr (S. Harzallah), mchabaat@usthb.dz (M. Chabaat), m.saidani@coventry.ac.uk (M. Saidani), mlmoussaoui@usthb.dz (M. Moussaoui).

https://doi.org/10.1016/j.cscm.2022.e01235
Received 20 April 2022; Received in revised form 30 May 2022; Accepted 10 June 2022
Available online 15 June 2022

and fast implementation make it an increasingly viable method. The composite reinforcement technique involves the bonding of fabric or plates made of steel, carbon or glass fibers to a concrete support [6]. The cement mortar matrix has a lower modulus of elasticity than glass, carbon, or steel. High modulus fibers can improve flexural strength and impact resistance at the same time. Fibers with a low elastic modulus such vegetable and polypropylene can improve the impact resistance of concrete but do not contribute much to its flexural strength [7–10].

Carbon fiber is a naturally occurring material with excellent mechanical characteristics [11–13]. Although carbon fibers are more expensive than glass fibers, they are increasingly becoming more employed in structures such as fiber reinforced concrete (FRP) wraps for strengthening or repairing RC columns, beams, and slabs [12]. The increasing use of carbon fibers due to their strength and high elastic modulus, their resistance to chemical, thermal and environmental effects, as well as their low density (low weight) makes them the ideal choice in cases where deflection and added weight are critical conditions [13]. Steel fibers have also been used for tensile reinforcement in concrete. They are discrete, short length and width of steel with a length-to-diameter ratio of 20–100, small enough to be easily and randomly dispersed in fresh concrete mix employing by ordinary mixture techniques [14,15].

Fiber reinforced concrete (FRC) is a composite material made up mostly of conventional concrete or mortar that has been reinforced by the random dispersion of short, discontinuous fine fibres of particular geometry. It was first proposed in 1910 [16], however, the first scientific research on FRC was carried out in 1963 [17]. SFRC is produced using the conventional hydraulic cements, fine and coarse aggregates, water, and steel fibers (SFs) [17]. It has been the subject of extensive research in the past [18–23]. A number of factors influence the beneficial effect of SFs in concrete, including type, length, shape, strength, cross section, fiber content, matrix strength, SFs binding strength, concrete mixing and mix design. The injection of SFs to conventional reinforced concrete (RC) members offers a number of benefits [24,25].

2. Damage detection by mathematical models using FEM

The analysis of damage in complex bridge structures is an important area of research because the focus is around the location of the cracking zones, following their propagation and finding adequate solutions [26,27]. The process of locating and detecting damage to the bridge using a limited number of responses recorded during strong earthquakes by the Updating Finite Element Model with the vibration-based system is very effective in assessing the damage under strong earthquakes [28,29].

The present study consists in carrying out a dynamic detection of damage in RC bridges using a method of improved mathematical models of finite elements from the measured data MMUM. An adapted finite element mesh of a repaired bridge was carried out [30,31]. The diagnosis helps to locate and detect areas of damage in the RC bridge. In addition, the centered finite difference scheme was developed to solve the system of equations for manipulating the finite element matrices of the bridge model. The method is to detect damages and existing cracks in real-time of a repaired bridge. Bridges are structures whose arrangement is horizontal, that is to say they are intended to work predominantly in flexion with respect to the horizontal with a displacement that is vertical unlike buildings whose arrangement is vertical. Kibboua [32,33] cited in his work the vulnerability of structures and how past research did not take into account the rigidity. In the present study, the rigidity is an important parameter as well as the structural mass and the masses due to the additional loadings. Additionally, structural damping is introduced and modeled to reproduce the real case of the response to vibrations.

3. Research novelty

This study is more rigorous since it is possible to predict the vulnerability of the structure by analyzing whether the admissible elastic stress of the composite materials is exceeded in the localized damage zones because the calculations involve structural rigidity, mass and damping. For reasons of unavailability of all the information relating to the parameters that can deteriorate the structure such as a natural disaster, it is possible to design the structure by a reliability calculation. This makes it possible to take into account these parameters by choosing for example a probability that considers the safety margin as a random variable.

In this research work, detection and prediction of damage zones using von Mises' criteria are numerically analyzed with the dynamic system of finite elements using equations that computes the dynamic response (Nonlinear Dynamic Analysis). The numerical analysis system can determine the dynamic displacements at each degree of freedom and the corresponding strains and stresses inside the elements under earthquake for each time-step iteration by dynamic finite element system. The analysis is carried out on a damaged and repaired bridge. The properties of RC materials use rules for mixing two basic materials, concrete and steel. Concrete composed of cement, gravel and sands is considered by researchers to be an isotropic paste with its known material properties. In addition, the RC resistance is formulated from concrete and steel reinforcement resistors with the introduced formula. Based on a steel frame arbitrarily located in the concrete structure, it is assumed that a tetrahedron element of arbitrary shape has the same properties as the properties of the bridge structure material and is considered to be a heterogeneous material compared to the whole modeled structure. It is important to note that this method can include the effects of reinforcement steel in RC properties [24]. Structural Rayleigh damping considered in this analysis includes the self-damping construction. It is an important parameter under severe dynamic loading of vehicles and potential earthquakes quantified with horizontal and/or vertical vibration. Obviously, damage and failures are a result of the fatigue behavior of cyclic stress.

4. Problem description and research solution

The bridge considered by the study was built in 1926. It suffered several cracks in the beams at the junction with the pillars or posts.

It was repaired where some details have been added to the model. The periodic maintenance includes reinforcement with CFC carbon fiber fabrics, injection with SikaDur 52 injection type epoxy resin, addition of SikaTop 126 type concrete, application of a protective stain and replacement of the gaskets of pavements. The mesh considered in this study is that of the bridge before the repair, based on the plans provided by the builder. Beyond this date, stiffeners and thin beams were added between the longitudinal beams as well as a mass of concrete between the pillars. The model turned out to be very loaded according to digital data, which is difficult to manipulate due to insufficient available computer memory. Therefore, it was assumed that stiffeners and thin beams do not have a significant effect on concrete beams. In addition, the concrete masses can only prevent the displacement of the pillars relative to them by imposing a common displacement for all the pillars of the same pile. Significant displacement can lead to a disaster as in the case of the Kobe earthquake.

The nonlinear dynamic analysis in real time (case where the measured data is directly transmitted to the calculation code) of this bridge will inform about its behavior at each measurement step as well as the exact areas with the degrees of freedom of the damage cases. The determination of a computer code to generate the stiffness, mass and overall damping matrices of finite elements has been carried out. A new efficient method for obtaining the shape or interpolation functions of the tetrahedral element with nodes and constant strain field has been introduced [34–36]. The program has allowed obtaining the interpolation functions of any non-degenerate element of the mesh. Nazé [37] developed a complex method that determines the level of acceptable risk using the definition of a damage indicator. This random variable must satisfy a few conditions to ensure a precise operation such that the damage is calculated in a complex way.

In this study, a method based on the probability of the safety margin that proved to be a good and efficient choice using the available mechanical stresses is presented. Ferreira [38] developed a matrix of the properties of the shell material in the two-dimensional plane of the element with a 3D representation due to the assembly of the elements with the use of a shear factor at rotational degrees of freedom. Ferdjani [39] carry out modeling of the matrix a properties of the orthotropic material with constants in two-dimensional. The membrane effects of traction (or compression) where the elements have no conventional representation for the case of prestressed concrete in the non-cracking state, such that the axes of orthotropy are oriented along the main axes.

The research work is a generalization of Hooke's law for the volume case. For this purpose, a tetrahedral element with three degrees of freedom per node was used, because its deformation is volumetric. A new form of the matrix properties of a volume anisotropic material was developed from the theory that exists in the two-dimensional literature on composite materials and for orthotropic material properties, with symmetry constants and planes, using the generalized Hooke's law. The calculations provided the property matrix of the concrete-steel mixture knowing that the concrete consists of cement, sand, gravel and other impurities on the volume case. The partitioning of the matrices and the discretization of the differential equation of motion was performed.

In a previous research work, the authors presented improved mathematical models using finite element methods that are cited in the references but these methods did not allow considering the structural damping. However, considering damping is essential as structures undergo a self-damping state after any form of vibration, such as those caused by dynamic loading or by earthquakes in the form of horizontal and/or vertical vibrations. For this reason, structural damping is included in this research.

5. Description of the structure

The bridge under consideration is a slab bridge with two continuous spans, and a pier of two columns. Figs. 1 and 2 show a longitudinal and a transverse section of the pier bridge. The total calculated weight of the bridge is 27850.36 kN.

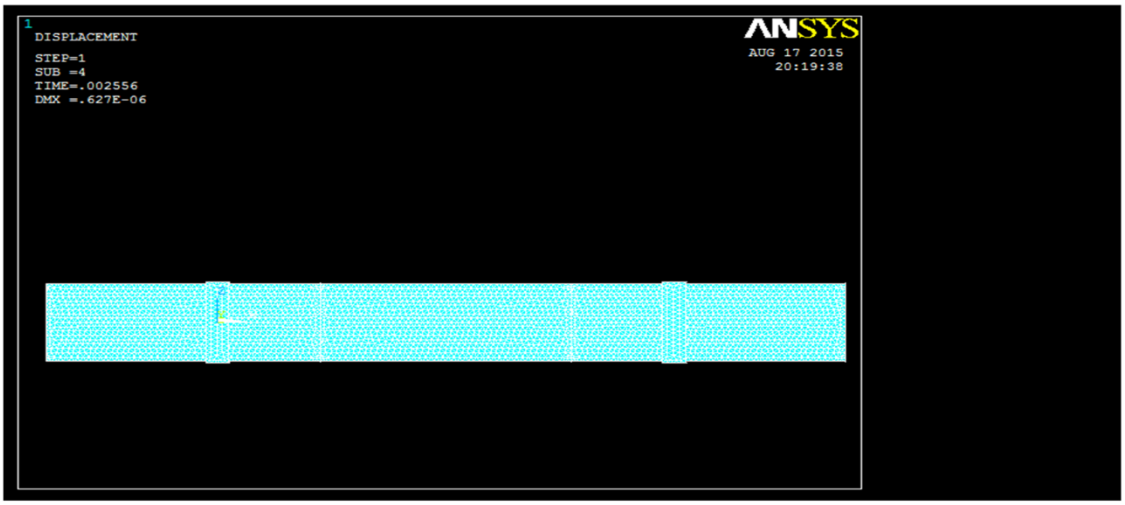

Fig. 1. Longitudinal section of the bridge.

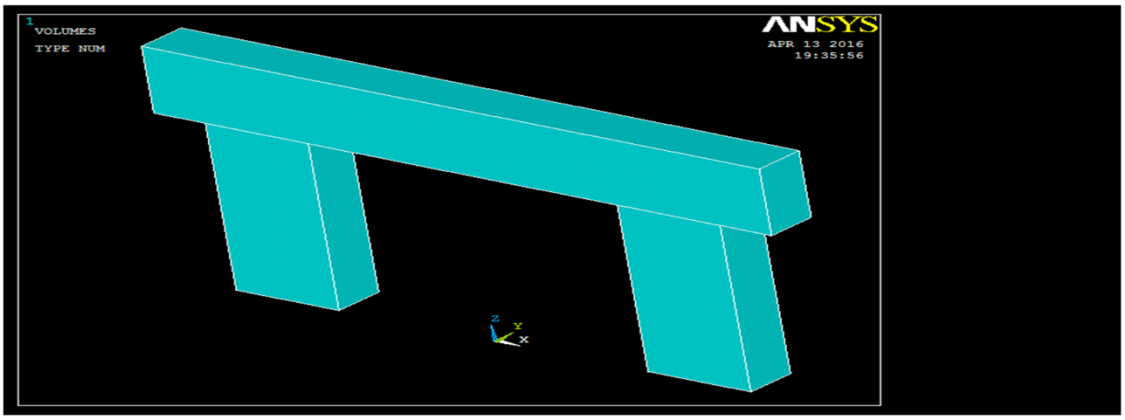

Fig. 2. Transverse section of the pier.

5.1. *Definition of materials*

The notion of fiber reinforcement was introduced in contemporary days and as best fibers were reinforced with brittle cement-based paste when the so-called Hatschek process was invented in around 1900 for the manufacture of roofing plates, pipes, etc. Glass fibers were later suggested for reinforcement by Biryukovichs [40] for cement paste and mortar. The ordinary E-glass fibers are not resistant and durable in highly alkaline Portland cement paste and the alkali resistant (AR) glass fibres with addition of zircon oxide ZrO2, were invented by Majumdar and Ryder [41]. Romualdi and Batson [42] and Romualdi and Mandel [43] published work on the advancement of steel fiber reinforced cements (SFRC).

The application of dispersed fibre reinforcement resulted in a wide range of excellent construction materials for numerous purposes-fibre reinforced cements and concretes (FRC) [44]. Since the material was made of any mixture and the discretization in tetrahedral elements being arbitrary, all the elements were assumed to have the same calculated properties. The reinforced concrete is mainly composed of two materials which are concrete (matrix m) and steel (fibers f) to form a mixture of materials. The law of mixtures makes it possible to establish properties using volume fractions [45].

Concrete is reinforced with steel bars such as fiber-like composite chips that include targeted fibers for each layer and are adding some fiber to the concrete matrix. Steel fiber bars are placed in the concrete matrix in the form of arbitrary; in addition, concrete is a paste of isotropic material [24].

Unidirectional fibers give the maximum properties in the direction of the fibres, corresponding to the case of the simple arrangement. Furthermore, they provide the minimum properties in the transverse direction. On the other hand, the law of mixtures is a good representation of the experiment. For this reason an analogy formulation was used by Ferreira [38] for the shell finite elements.

The composite reinforced concrete strength for the bridge structure is given as follows:

$$S_{rc} = (v_f + v_m \frac{E_m}{E_f}) \tag{1}$$

Eq. (1) includes the effects of steel reinforcement in the concrete structure. The material strength stresses are given in Table 1 where S_f is the steel yield strength, S_m is the concrete yield strength and S_{rc} is the RC [46,47].

Volume fractions of steel fibers (f) and volume fractions of concrete matrix (m) are related as follows:

$$\mathrm{v_m} + \mathrm{v_f} = 1 \tag{2}$$

where; v_m and v_f are the concrete and steel volume fractions, respectively.

Let $\mathrm{V_f}$ the volume of steel, $\mathrm{V_m}$ the volume of concrete and $\mathrm{V_{rc}}$ the volume of reinforced concrete:

$$\mathrm{v_f} = \frac{\mathrm{V_f}}{\mathrm{V_{rc}}} \tag{3}$$

Table 1
Characteristics of fiber and matrix mixture.

Characteristics of fiber and matrix mixture							
E_m [MPa]	E_f [MPa]	G_m [MPa]	G_f [MPa]	ρ_m [kg/m^3]	ρ_f [kg/m^3]	v_m	v_f
30798	207000	12319	80233	2402.8	7850	0.25	0.29
Characteristics of reinforced concrete and steel				Characteristics of the mixture of materials			
V_{rc} [m^3]	V_f [m^3]	M_{rc} [kg]	M_f [kg]	E_{rc} [MPa]	v_{rc}	ρ_{rc}[kg/m^3]	G_{rc} [MPa]
410.76	7.849	$10.28 * 10^3$	61614	34165	0.2508	2506.87	12522

$$v_m = \frac{V_m}{V_{rc}} = 1 - v_f \tag{4}$$

The mechanical properties of matrix materials [D− 1] (6 × 6) are expressed in terms of the properties of heterogeneous materials RC from Hooke's general law under the following form;

$$\begin{pmatrix} \varepsilon_{xx} \\ \varepsilon_{yy} \\ \varepsilon_{zz} \\ \varepsilon_{yz} \\ \varepsilon_{zx} \\ \varepsilon_{xy} \end{pmatrix} = \begin{pmatrix} \frac{1}{E_{rc}} & -\frac{v_{rc}}{E_{rc}} & -\frac{v_{rc}}{E_{rc}} & 0 & 0 & 0 \\ -\frac{v_{rc}}{E_{rc}} & \frac{1}{E_{rc}} & -\frac{v_{rc}}{E_{rc}} & 0 & 0 & 0 \\ -\frac{v_{rc}}{E_{rc}} & -\frac{v_{rc}}{E_{rc}} & \frac{1}{E_{rc}} & 0 & 0 & 0 \\ 0 & 0 & 0 & \frac{1}{2G_{rc}} & 0 & 0 \\ 0 & 0 & 0 & 0 & \frac{1}{2G_{rc}} & 0 \\ 0 & 0 & 0 & 0 & 0 & \frac{1}{2G_{rc}} \end{pmatrix} \begin{pmatrix} \sigma_{xx} \\ \sigma_{yy} \\ \sigma_{zz} \\ \sigma_{yz} \\ \sigma_{zx} \\ \sigma_{xy} \end{pmatrix} \tag{5}$$

where;E_{rc} and v_{rc} correspond to the Young's modulus and Poisson's ratio, respectively. G_{rc} is the.
shear modulus.

$$\begin{Bmatrix} E_{rc} = E_m v_m + E_f v_f \\ v_{rc} = V_m v_m + V_f v_f \\ \rho_{rc} = \rho_m v_m + \rho_f v_f \\ \frac{1}{G_{rc}} = \frac{v_m}{G_m} + \frac{v_f}{G_f} \end{Bmatrix} \tag{6}$$

For the case of the Oued Oumazer bridge, data considered in this study are listed in the following Table 1.

5.2. Definition of elements cross-section

Table 2 gives the dimensions of the sections of bridge piers also represented graphically in Fig. 3.

6. Nonlinear dynamics analysis

Consider that Bridge Piers is subjected to the earthquake of Boumerdes (Algeria) which is classified by the RPA 99/version2003 (CGS, 2003) as zone III (very high seismicity). The response spectrums on the displacement (a), in pseudo speed (b) and in pseudo acceleration taken from [48]. Fig. 4 shows the 2003 Boumerdes earthquake accelerogram of the response spectrum conversion in acceleration to a spectrum of demand.Fig. 5.

The tetrahedral mesh characteristics of the analyzed bridge piers structure shown in Fig. 4 are the number of degrees of freedom (dof) equals to 45,927, the number of tetrahedral 45,352, and the number of nodes 15,309. Computed Ansys principal stresses allow determination of the dynamic stresses, to verify if the RC strength bound is satisfied. It is important to notice that this dynamic analysis requires several time steps computations and handles large matrices of 45,927 dof. A total of 12 Ansys batch files for each simulation case have been carried out. The results in Figs. 6–13 show a graphical evolution of the dynamic solution.

The meshing process and the solution are carried out using the Ansys finite element software. It is important to notice that the necessary time to mesh the structure is not included in the available CPU times on the analysis time range. The generated meshes are stored for use in the Ansys commands batch files, summarizing the participation rate of the modal masses, where the first three modes of participation rates of the most important masses are taken into consideration.

The analysis below shows the development of plastic hinges, Von Mises stresses and deformations such that each provides

Table 2
Transverse sections of elements.

Elements	b (m)	h (m)	d (m)	A (m^2)	I (m^4)
crosshead	1.9822	1.8268	_	3.6142	1.0178
columns	_	_	1.527	1.8229	0.2656

where; b is the width of the crosshead, d is the diameter of columns, I is the moment of inertia, H the height of the crosshead, A the area of the element, and W = 576.43 kN/ml

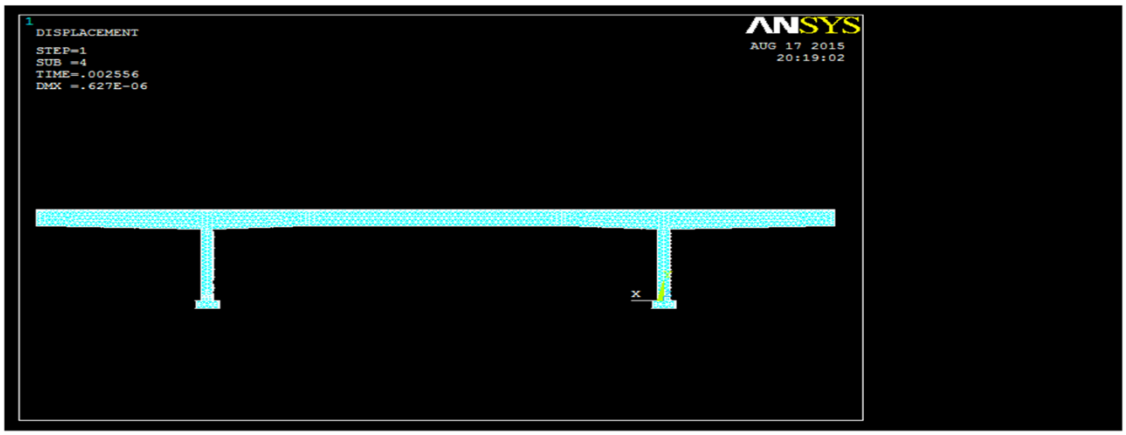

Fig. 3. Overall plan and view of the bridge.

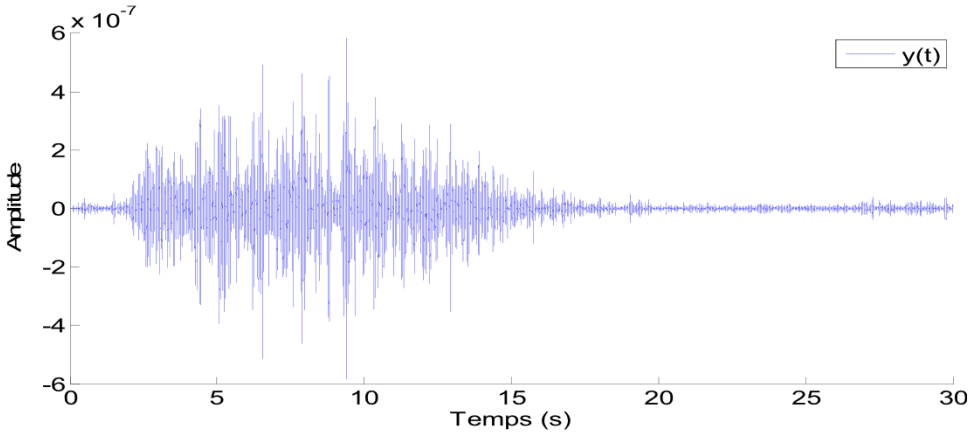

Fig. 4. Earthquake accelerogram May 21, 2003 Boumerdes, Algeria [16].

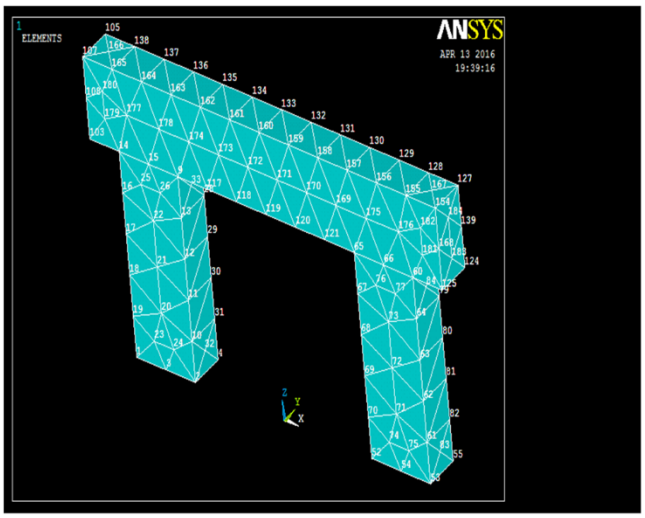

Fig. 5. Mesh of Bridge Piers.

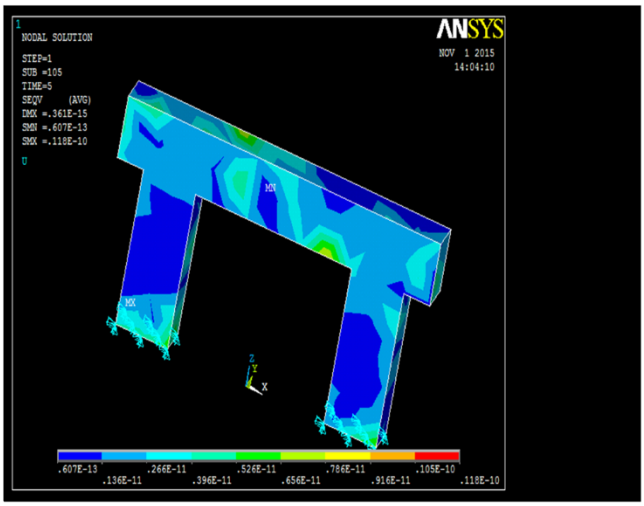

Fig. 6. Deformation-sum resulting from step 1.

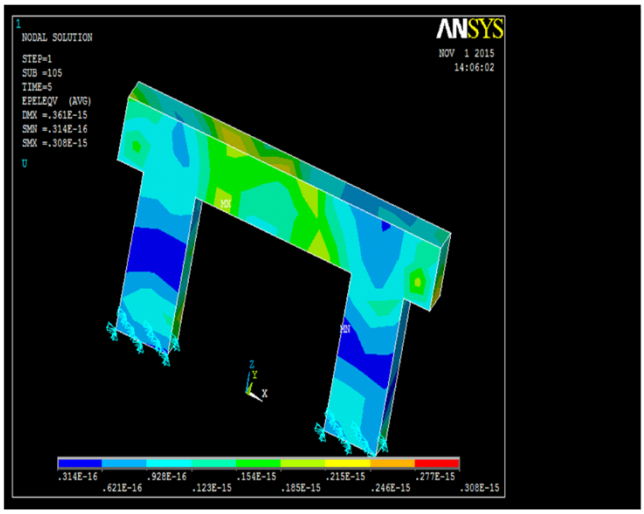

Fig. 7. Deformation-sum and cracking of concrete at the bottom of element 2 resulting from step 19.

amplitudes and the corresponding time period and solution subset. The first and the last series set of solutions were saved. To prevent the problem of storing data and big data, it is necessary to ignore past results and only save the results that correspond to the time stages. This program gives results in each time step without the previous steps. That is, it does not display the time series.

The computed principal stresses from Ansys allows obtention of the equivalent Von Mises, to check whether the RC strength bound is adequate. It is necessary to remember that this complex study involves computations at different time stages involving 45,927 degrees of freedom. In summary, 12 Ansys files are generated for each simulation scenario.

Composite laminates have different failure criteria. As the study is carried out with a heterogeneous material, the Von Mises failure criterion has been chosen using the equivalent stress in the element and fulfilling the RC strength bound by satisfying the resistance requirement.

$$\sigma_{equiv} < S_{rc} \tag{7}$$

$$\sigma_{equiv} = \sqrt{\frac{1}{2}\left(\quad (\sigma_1 - \sigma_2)^2 + (\sigma_2 - \sigma_3)^2 + (\sigma_3 - \sigma_1)^2 \right)} \tag{8}$$

The finite element Ansys software was used to determine the elastic Von Mises equivalent strain and stress.

From the results obtained, it is clear that the Von Mises equivalent stress is greater than the strength of reinforced concrete, generating fractured regions when wearing the joint. It clearly demonstrates that cyclic stresses and earthquakes at the bedam-column connections can generate sensitive crack zones. On the other hand, maximum stresses which exceed the material ultimate stress,

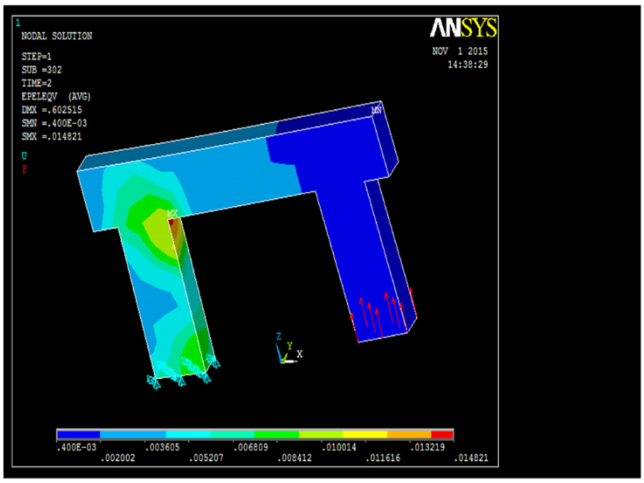

Fig. 8. Deformation-sum and Development of plastic hinges at the bottom of element 4 resulting from step181.

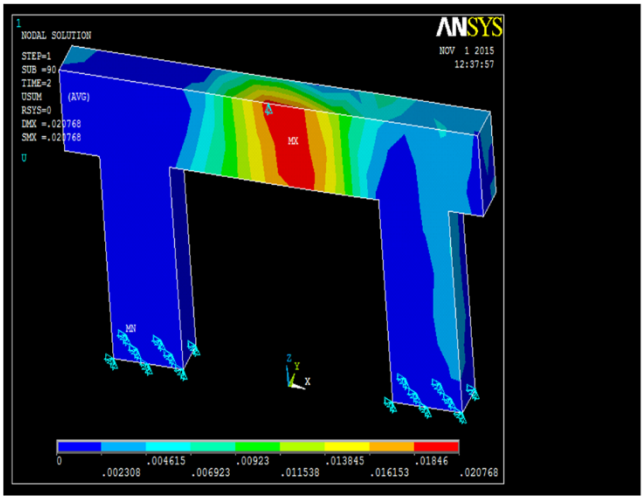

Fig. 9. Deformation-sum and Development of plastic hinges resulting from step 183.

appear at the intersection and at the fixings in the model, where dynamic movement takes place. This is due to the severe loading case chosen in this application which graphically shows the dynamic behavior of the frame. However, it is clear that in the entire structure of the bridge that the neoprene, originally designed as shock absorbers, was damaged. This is due to the bending effect resulting in shearing of this material. The contact is linear at the level of the lower part of the beams with a variable section which is the main cause for the Neoprene to be crushed linearly. Besides, the wear of the neoprene causes the beams to damage the columns, resulting in the appearance of cracked areas. As is well known and shown by this study, earthquakes and cyclic stresses can generate cracking zones at beam-column joints.

According to the finite element analysis, the highest stress obtained by the equivalent stresses of Von Mise is close to the material yield limit, meaning near the damage zone. When the bridge's frame platform is subjected to a substantial dynamic stress, the crack will gradually propagate from inside to outside, leading eventually to the fracture of the frame. The beam-column connection has a lot of cracks, according to analysis of the microstructures.

It is obvious that in the case of severe loads, the von Mises equivalent stress is greater than the strength of RC. This stress can generate fractured regions when wearing the joint. This research study clearly demonstrates that cyclic stresses and earthquakes at the connections beams-columns can generate sensitive crack zones. The results obtained from this research are in good agreement with the predicted value based on the ideal failure criterion and correspond to the damage zones.

According to the critical results of previous numerical studies, addition of steel fibers inside the concrete medium enhances the peak strength reached by specimens during dynamic loading as compared to before the bridge repairs.

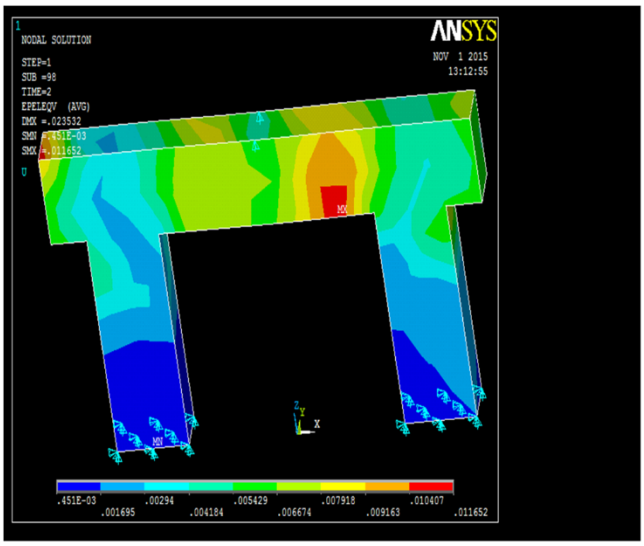

Fig. 10. Deformation-sum and Development of plastic hinges at element 4 resulting from step 186.

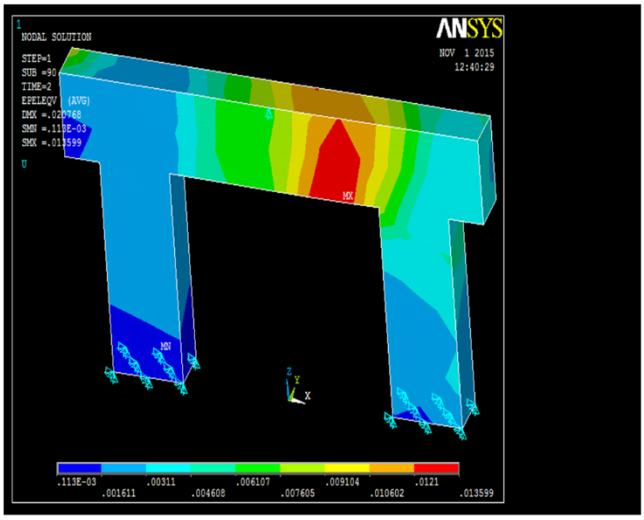

Fig. 11. Deformation-sum and Development of plastic hinges at element 3 resulting from step 189.

6.1. *Nonlinear analysis of RC sections (M - φ)*

The nonlinear behavior of structures beyond their elastic phase depends on the materials constituting their structural elements. Reinforced concrete exhibits a non-linear behavior due to the cracking and crushing as well as plasticization of the steel. These nonlinearities can be considered by laws of behavior. It is necessary before a nonlinear computation is carried out to carry out a nonlinear analysis of the sections to determine its laws of behavior. Results of the nonlinear analysis (M-φ) obtained by Ansys are shown below for two different sections (crosshead and column) of the bridge.Fig. 14 and 15.

6.1.1. *Crosshead*

The curve M-φ is not symmetrical since the distribution of reinforcement on the section is not (stretched frames ‡ compressed frames). Otherwise, Fig. 16 below represents the simplified tri-linear curve M-φ and values of interest are given in Table 3 below.

6.1.2. *Columns*

It is worth noting that the normal effort N has an influence on M–φ and that columns have different values of N. The curve M-φ is symmetrical because the distribution of reinforcement on the section is symmetrical. Fig. 17 represents the simplified trilinear curve of M–φ of the elements 1 and 2.Table.4.

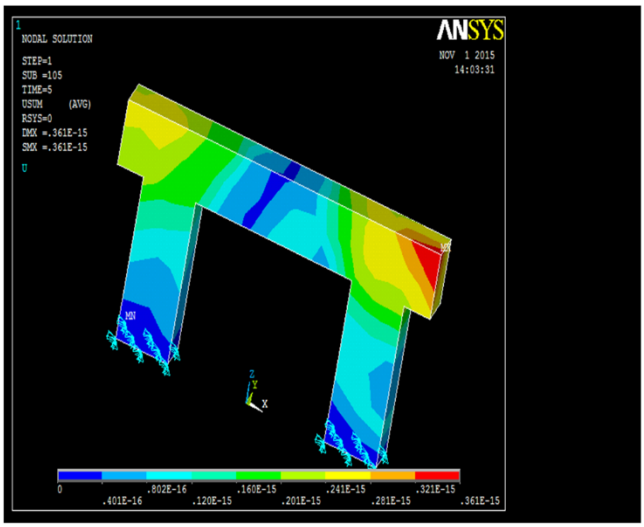

Fig. 12. Deformation-sum and Development of plastic hinges at element 3 resulting from step 192.

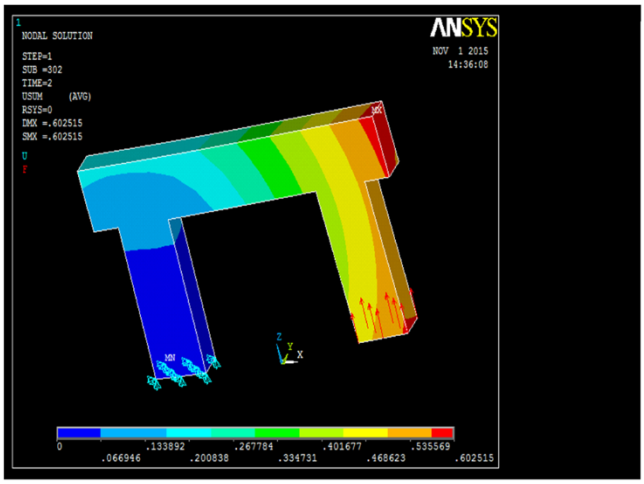

Fig. 13. Deformation-sum and Development of.

6.2. Capacity curve and degradation of structural stiffness

The capacity curve of a structure represents the horizontal force at the base of the building as a function of displacement. In general, it is made of a linear elastic phase followed by a non-linear phase corresponding to the formation of the flexural and shear hinges, until the moment of rupture.

Fig. 18 represents the curves of capacity and development of plastic hinges obtained by a Pushover analysis. It illustrates the difference between the two capacity curves (with and without P-Δ). One can notice that the compatibility of the two curves fit up to a threshold (see the point indicated in the figure) and afterwards, a separation of the curves explains the influence of P-Δ on the behavior. Table 5 gives the ductility of the two curves.

7. Comments and observations

Table 6 summarizes the state of bridge piers during loading steps (see Fig. 18).

Fig. 18 illustrate the behavior that is closer to the real behavior of the structure in question. These curves are characterized initially by an elastic part containing the cracking of the concrete up to the elastic limit designated by the first point of plasticity of the steels then they increase while describing the behavior of the structure in its inelastic phase, finally, a significant degradation of the lateral stiffness Bridge Piers is observed until the rupture is reached by a formation of a failure mechanism. The maximum displacement associated with the rupture is equal to 3.82 cm corresponding to the ultimate lateral displacement of Bridge Piers.

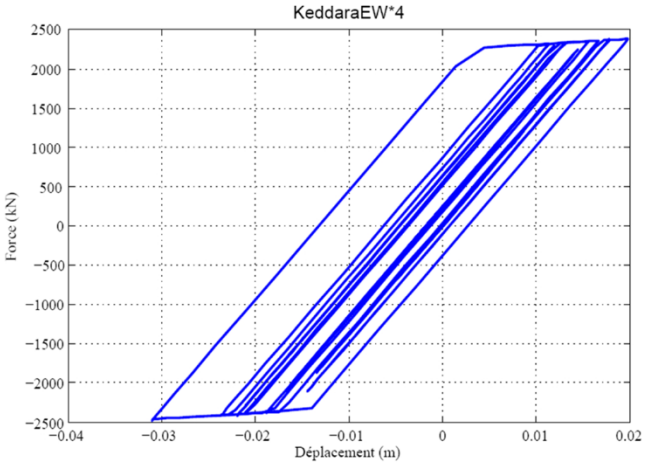

Fig. 14. Results of nonlinear dynamic analysis.plastic hinges at element 3 and 5resulting from step 201.

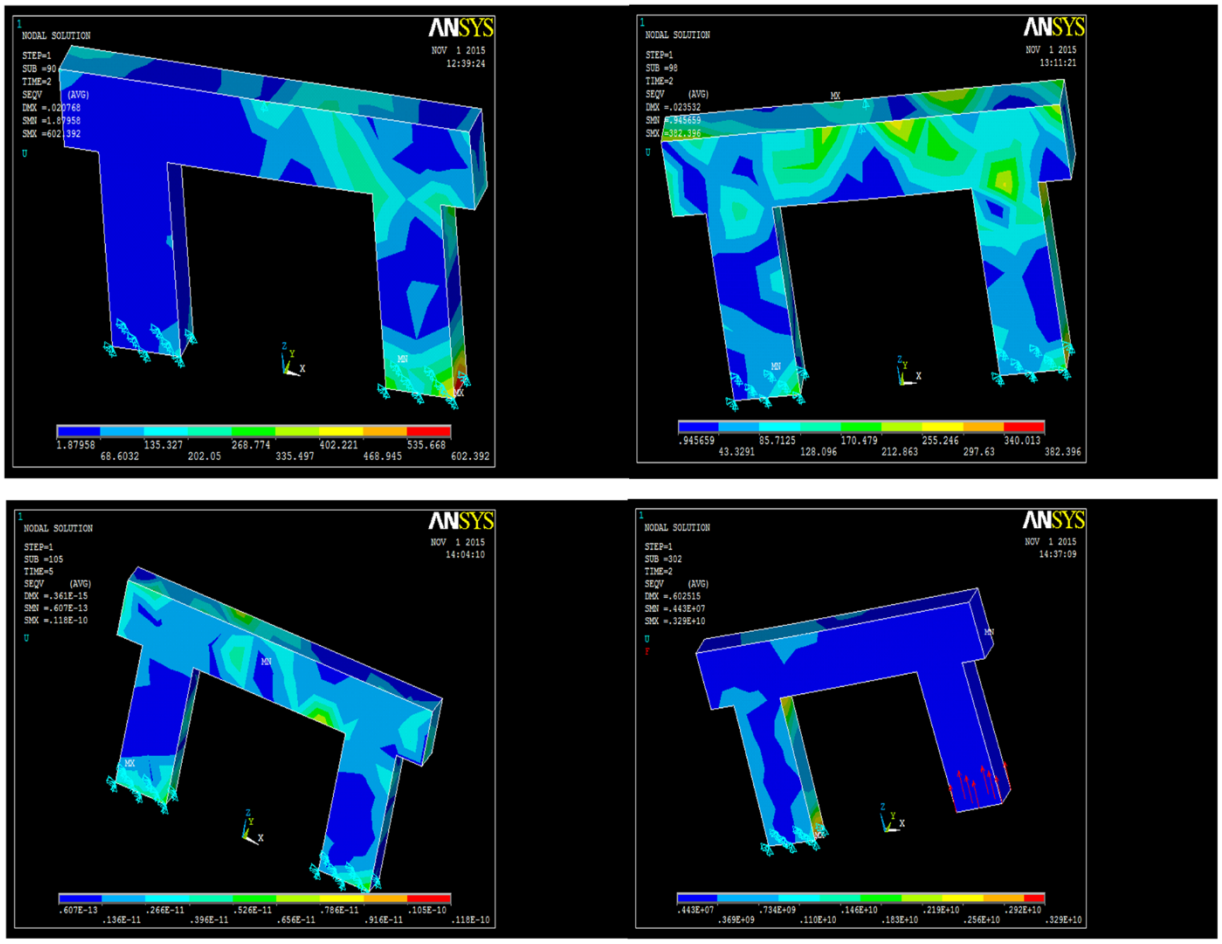

Fig. 15. VonMisesstressesofmodelinthe first and lastsetsolution(series 1,2,3and4).

8. Performance point during the BOUMERDES earthquake

Fig. 18 shows the superposition of demand spectrum and capacity spectrum, as well as the bilinear capacity spectrum representation. To estimate the earthquake strain and find the point of performance (Fig. 18), the steps of ATC procedure A were followed.Fig

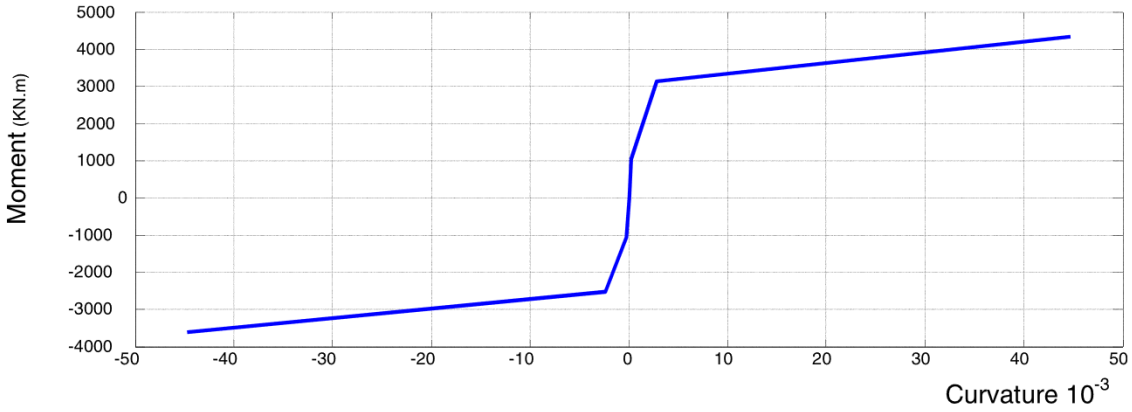

Fig. 16. Moment-curvature tri-linear (simplified).Crosshead.

Table 3
Moment-curvature values of interesting events (crosshead).

	Curvature (1/m) 10^{-3}	Moment (kNm)
Cracking of the concrete (-)	-0.274	-1036
Plastic frames (-)	-2.330	-2530
Ultimate state (-)	-44.717	-3608
Cracking of the concrete (+)	0.274	1054
plastic frames (+)	2.819	3143
Ultimate state (+)	44.717	4343.6

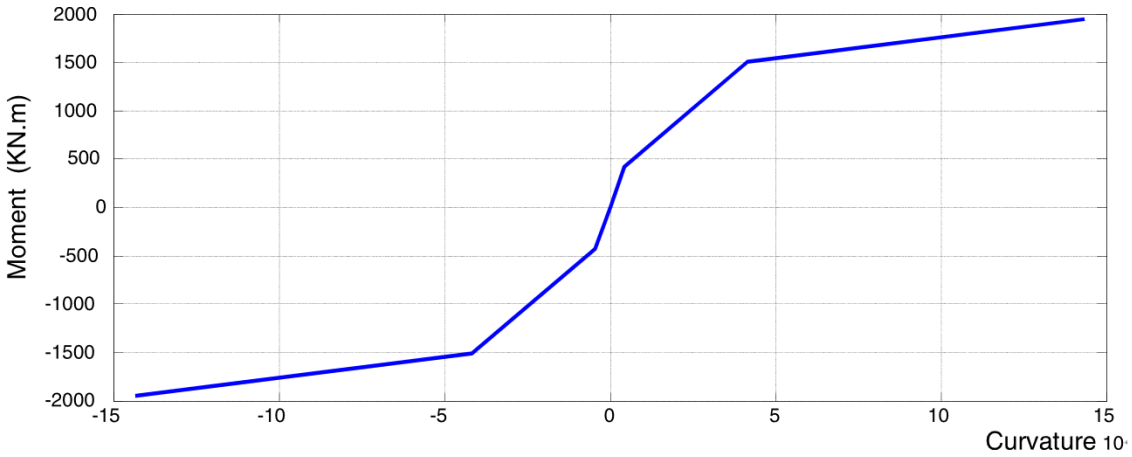

Fig. 17. Moment-curvature tri-linear (simplified) of the element 1, 2.

Table 4
Values moment-curvature of interesting events (Columns).

	Curvature (1/m) 10^{-3}	Moment (kNm)
Cracking of the concrete (-)	-0.438	-0424.0
Plastic frames (-)	-04.155	-1512.0
Ultimate state (-)	-14.344	-1949.9
Cracking of the concrete (+)	0.438	0424.0
Plastic frames (+)	04.155	1512.0
Ultimate state (+)	14.344	1949.9

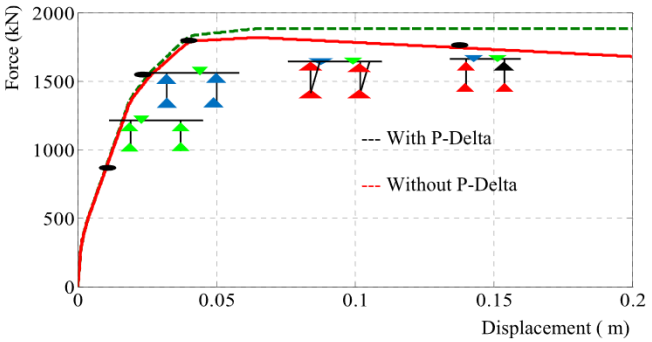

Fig. 18. Curve of capacity and condition of plastic hinges with and without P-Δ.

Table 5
Ductility of two curves with and without P-Δ.

	Dy (mm)	Fy (kN)	Du (mm)	Fu (kN)	μ
with P-Δ	11.91	9323.075	35.44	13072.68	2.98
without P-Δ	11.91	9359.857	35.2	13187.88	2.95

Where, Dy: Displacement at the summit for the first plastification of steels.
Du: Ultimate displacement at the summit.
Fy: Strength at the base for the first plastification of steels.
Fu: Ultimate strength at the base, μ: Ductility.

Table 6
Summary of the results.

Steps	Displacement (mm)	Strength (kN)	Stiffness (kN/m)	Cumulative observations
1	0,0097	0,00	850,515464	/
13	1202	271,00734	225,463677	Appearance of the first hinge in B–IO range
16	1502	326,789718	217,569719	Cracking of concrete at the top of elements 5
17	1602	342,391749	213,727684	Cracking of concrete at the left of element 2
24	2302	390,26974	169,535074	Cracking of concrete at the bottom of element 4
38	3702	490,927089	132,611315	Cracking of concrete at the top of element 4
185	18,402	1321,43867	71,8095136	Appearance of the first hinge in IO–LS range
187	18,602	1330,71591	71,5361741	Plasticizing of steels at the top of element 5
204	20,302	1390,7651	68,5038469	Plasticizing of steels at the bottom of element 5
263	26,202	1537,81371	58,6906996	Plasticizing of steels at the bottom of element 4
366	36,502	1725,18144	47,2626552	Plasticizing of steels at the top of element 4
396	39,502	1773,13139	44,8871295	Plasticizing of steels at the left of element 2
399	39,802	1777,23945	44,6520137	Appearance of the first hinge in LS–CP range
403	40,202	1782,72364	44,344153	Crushing of concrete at the bottom of element 5
425	42,402	1794,57239	42,3228242	Crushing of concrete at the bottom of element 4
650	64,902	1818,48445	28,0189278	Crushing of concrete at the top of element 4
1818	181,702	1698,72165	9,34894305	Appearance of the first hinge in collapse range
1840	183,902	1696,45945	9,22480152	Rupture of Bridge Piers
1875	187,402	1692,86049	9,03331069	Rupture of Bridge Piers
2000	199,902	1680,00709	8,40415349	Collapse

19 and 20.

From Fig. 18, it can be seen that bridge remains in the plastic domain (before the plastification of steels). However, the state of damage of the concrete is more advanced as is evident from the visible cracks at the top and bottom of the columns and the crosshead as shown in Figs. 6–14. These figures clearly show the damaged state of bridge.

The nonlinear calculation makes it possible to follow the behavior of structures beyond their elastic state. This type of assessment has the advantage of taking into consideration the degradation of the rigidity of the elements constituting the structure and consequently, the redistribution of the internal forces. The new techniques of verification and design of structures in reinforced concrete are based on performance objectives and develop appropriate preliminary designs, evaluate the seismic demand and the capacity of the structure to be checked if the design satisfies the main goal. According to the Performance-based seismic design (PBSD) method, the behavior assessment allows evaluation and verification of the performance of a structure subjected to an earthquake.

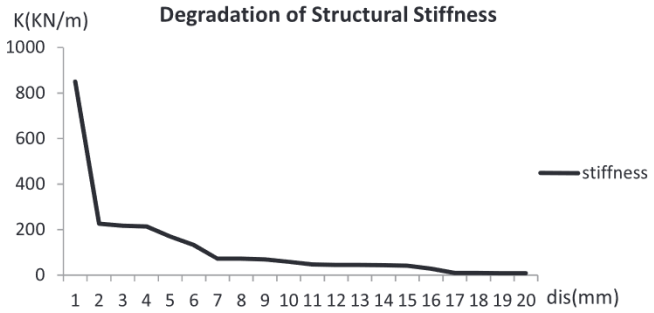

Fig. 19. Degradation of Structural Stiffness.

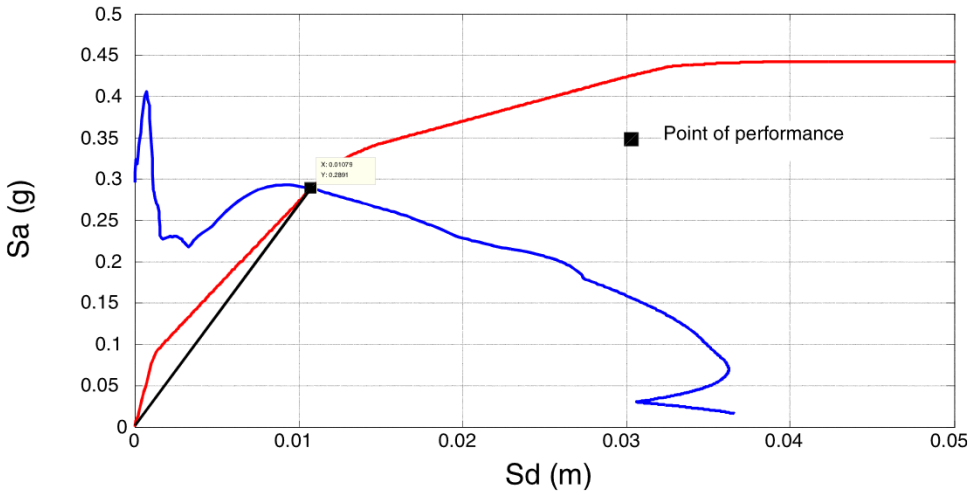

Fig. 20. Evaluation of the BB2 performance point for the Boumerdes earthquake ($\xi = 21.9\%$).

9. Conclusion

The research presented a repair and maintenance method of a bridge under dynamic loading that included reinforcement with carbon fiber composite (CFC) and steel fiber reinforced concrete (SFRC), injection with Sikadur 52 injection type epoxy resin, and addition of Sikatop 126 type concrete. The mechanical features, benefits, and uses of SFRC and carbon fiber fabrics were analyzed. Concrete technology has progressed tremendously during the previous few decades. Fibre Reinforced Concrete (FRC) is described herein as a composite material consisting of conventional concrete reinforced by the random dispersal of short, discontinuous fine fibres of particular geometry. Accordingly, the study focused on the numerical analysis of the behavior of SFRC and CFC by the finite element method for regeneration and repair of bridges under dynamic loading rates in order to determine the nature and extent of failure based on comprehensive numerical assessment using Von Mises' criteria.

Steel fibres are used to reinforce concrete, resulting in durable concrete with excellent fatigue and flexural strength properties, as well as the impact and spalling resistance of an improved abrasion. The reduction of conventional reinforcing as well as in some conditions, a reduction in section thickness, can result in significant productivity gains. Steel fibers can save money by reducing material volume, speeding up the construction process, and lowering labor expenses. As a result, steel fibers are considerably a more cost-effective design option. Steel fibres in concrete are distributed randomly, providing crack-free stress tolerance all through the concrete. As a result, micro cracks are identified before they develop and affect the concrete's performance.

This study allowed better understanding of the concepts of damage detection by locating cracking zones through identification with degrees of freedom. It also allowed generation of an efficient computer code for the processing of tetrahedral finite elements and to generate the global finite element matrices of the whole structure in the sparse-by-assembly form. The method for the discretization and the partition of the system of dynamic equations led to a form of linear resolution using computational algorithms for sparsely divided matrices. The method also allowed determination of unmeasured degrees of freedom based on a small number of measured degrees of freedom data. The resolution of the dynamic problems using the Ansys software permitted to overcome the memory limitations on the available computer hardware. The results of the models showed that the strength of the reinforced concrete is satisfied since the same material properties of the real bridge are applied to the simplified model of the gantry.

Declaration of Competing Interest

The authors declare that they have no known competing financial interests or personal relationships that could have appeared to influence the work reported in this paper.

Acknowledgement

The authors acknowledge the Built Environmental Research Laboratory of the University of Sciences and Technology Houari Boumediene (USTHB) and the General Direction of Scientific Research and Development of Technology of the Ministry of Higher Education and Scientic Research in Algeria for kindly supporting this research.

References

[1] R. Joan, Casas, John James Moughty, Bridge damage detection based on vibration data: past and new developments, Front. Built Environ. (2017), https://doi.org/10.3389/fbuil.2017.00004.
[2] M.L. Moussaoui, M. Chabaat, Numerical analysis of damage zones in a bridge, Int. J. Struct. Integr. Vol. 11 (1) (2020) 1–12, https://doi.org/10.1108/IJSI-03-2019-0017.
[3] Elahinia, Mohammad, Mirzaee, Akbar, Shayanfar, Mohsenali, Abbasnia, Reza, Damage Detection of Bridges Using Vibration Data by Adjoint Variable Method; 2014,Shock and Vibration- Hindawi Publishing Corporationhttps://doi.org/10.1155/2014/698658.
[4] P. Pastorek, P. Novák, P. Kopas, M. Močilan, Finite element analysis of bond behavior in a steel reinforced concrete structure strengthened carbon fibre reinforced, Polym. (Cfrp) Strips Metal. vol. 56 (2017).
[5] Zhao Minglei, Li Jie, Xie Yi Min, Effect of vibration time on steel fibre distribution and flexural behaviours of steel fibre reinforced concrete with different flowability, case studies in construction, Materials 16 (2022), https://doi.org/10.1016/j.cscm.2022.e01114.
[6] Omar Al. Hattamleh Samer Rabab'ah, Bilal Abu Alfoul Hussein Aldeeky, Effect of glass fiber on the properties of expansive soil and its utilization as subgrade reinforcement in pavement applications, Case Stud. Constr. Mater. 14 (2021), https://doi.org/10.1016/j.cscm.2020.e00485.
[7] K.ürşad Atila Kumbasaroglu, Hakan Yalciner, Ahmet I. Yalciner, Alper Turan, Celik,Effect of polypropylene fibers on the development lengths of reinforcement bars of slabs, Case Stud. Constr. Mater. 15 (2021), https://doi.org/10.1016/j.cscm.2021.e00680.
[8] Huiming Zheng Kai Wu, Feng Chen Nan Shi, Jianan Xu, Analysis of the bond behavior difference in steel and steel fiber reinforced concrete (SSFRC) composite member with circular section, Constr. Build. Mater. 264 (2020), 120142, https://doi.org/10.1016/j.conbuildmat.2020.120142.
[9] Mateusz Dudek Krzysztof Ostrowski, Łukasz Sadowski, Compressive behaviour of concrete-filled carbon fiber-reinforced polymer steel composite tube columns made of high performance concrete, Compos. Struct. 234 (2020), 111668, https://doi.org/10.1016/j.compstruct.2019.111668.
[10] Rajai Z. Al-Rousan, Failure Analysis of Polypropylene Fiber Reinforced Concrete Two-Way Slabs Subjected to Static and Impact Load Induced by Free Falling Mass, Latin American Journal of Solids and Structures https://doi.org/10.1590/1679–78254895.
[11] Rajai Z. Al-Rousan, Mohammad A. Alhassan, Esmail A. AlShuqari, Behavior of plain concrete beams with DSSF strengthened in flexure with anchored CFRP sheets—effects of DSSF content on the bonding length of CFRP sheets, Case Stud. Constr. Mater. 9 (2018), https://doi.org/10.1016/j.cscm.2018.e00195.
[12] Rajai Z. Al-Rousan, Behavior of macro synthetic fiber concrete beams strengthened with different CFRP composite configurations, J. Build. Eng. 20 (2018), 595-608,ISSN 2352-7102,https://doi.org/10.1016/j.jobe.2018.09.009.
[13] Rajai Al-Rousan Mohammad Alhassan, Ayman Ababneh, Flexural behavior of lightweight concrete beams encompassing various dosages of macro synthetic fibers and steel ratios, Pages 280-293,ISSN 2214-5095, Case Stud. Constr. Mater. 7 (2017), https://doi.org/10.1016/j.cscm.2017.09.004.
[14] Xiaoshan Lin Lei Yang, Huiyun Li, J. Rebecca, Gravina,A new constitutive model for steel fibre reinforced concrete subjected to dynamic loads, Compos. Struct. 221 (2019), 110849, https://doi.org/10.1016/j.compstruct.2019.04.021.
[15] Colin D. Johnston, Steel fibre-reinforced concrete - present and future in engineering, construction, Composites 13 (2) (1982) 113–121, https://doi.org/10.1016/0010-4361(82)90047-7.
[16] A.E. Naaman, Fiber reinforcement for concrete, Concr. Int. 7 (1985) 21–25.
[17] J. Romualdi, G. Baston, Mechanics of crack arrest in concrete with closely spaced reinforcement. Journal of the Engineering Mechanics Division EM3, Proc. Am. Soc. Civ. Eng. 89 (1963), 147-168.
[18] ACI PRC-544.1R-96: Report on Fiber Reinforced Concrete (Reapproved 2009).
[19] American Concrete Institute (ACI), ACI 318-08: Building Code Requirements for Structural Concrete and Commentary, American Concrete Institute,, Farmington Hills, MI, 2008.
[20] Xiaoshan Lin Lei Yang, Huiyun Li, J. Rebecca, Gravina, A new constitutive model for steel fibre reinforced concrete subjected to dynamic loads, Compos. Struct. Vol. 221 (2019), 110849, https://doi.org/10.1016/j.compstruct.2019.04.021.
[21] Yaoyao Zhang Xiaojing Li, Xudong Chen Chong Shi, Experimental and numerical study on tensile strength and failure pattern of high performance steel fiber reinforced concrete under dynamic splitting tension, Constr. Build. Mater. 259 (2020), https://doi.org/10.1016/j.conbuildmat.2020.119796.
[22] Erfan Shafei Tohid Mousavi, Impact response of hybrid FRP-steel reinforced concrete slabs, Structures 19 (2019), https://doi.org/10.1016/j.istruc.2019.02.013.
[23] Degao Zou Yongqian Qu, Jingmao Liu Xianjing Kong, Xiang Yu Yu Zhang, Seismic damage performance of the steel fiber reinforced face slab in the concrete-faced rock fill dam, Soil Dyn. Earthq. Eng. 119 (2019) 320–330, https://doi.org/10.1016/j.soildyn.2019.01.018.
[24] Grzybowski, M.1989, Determination of Crack Arresting Properties of Fiber Reinforced Cementitious Composites, Chapter 12, Royal Institute of Technology, Stockholm, Sweden.
[25] M. Grzybowski, S.P. Shah, Shrinkage cracking of fiber reinforced concrete, Acids Mater. J. (1990) 87.
[26] S.R. Shiradhonkar, Manish Shrikhande, Manish Shrikhande, Seismic damage detection in a building frame via finite element model updating, Comput. Struct. 89 (23–24) (2011) 2425–2438, https://doi.org/10.1016/j.compstruc.2011.06.006.
[27] Zhenhuan Song Rongxin Zhou, Yong Lu, 3D mesoscale finite element modelling of concrete, Comput. Struct. 192 (2017), https://doi.org/10.1016/j.compstruc.2017.07.009.
[28] Yu-Wei Wei, Jia-Feng Lai, Xiao-Bing Sun, Ji-Peng Liu, Da-Zhen Tan, Hai-Bo Ye, Hua-Lin Chen, Jie Lu, Ji-Le Chen, An-Xiao Peng, Fracture failure analysis and finite element assessment of bridge detection vehicle, Eng. Failure Anal. 125 (2021), https://doi.org/10.1016/j.engfailanal.2021.105423.
[29] Siti Shahirah Saidin, Sakhiah Abdul Kudus, Adiza Jamadin, Muhamad Azhan Anuar, Norliyati Mohd Amin, Zainah Ibrahim, Atikah Bt Zakaria, Kunitomo Sugiura, Operational modal analysis and finite element model updating of ultra-high-performance concrete bridge based on ambient vibration test, Case Studies in Construction Materials,Volume 16,2022,https://doi.org/10.1016/j.cscm.2022.e01117.
[30] Mohammad A. Alhassan, Rajai Z. Al-Rousan, Layla K. Amaireh, Muneer H. Barfed, Nonlinear finite element analysis of B-C connections: influence of the column axial load, jacket thickness, and fiber dosage, Structures 16 (2018), 50-62,ISSN 2352-0124,https://doi.org/10.1016/j.istruc.2018.08.011.
[31] Z. Rajai, Al-Rousan, Empirical and NLFEA prediction of bond-slip behavior between DSSF concrete and anchored CFRP composites, Constr. Build. Mater. 169 (2018), 530-542, ISSN 0950-0618,https://doi.org/10.1016/j.conbuildmat.2018.03.013.
[32] Kibboua A., Développement d'une méthodologie d'analyse pour la vulnérabilitésismique des piles de ponts Algériens, Thèse de Doctorat en Génie Civil, USTHB, Algérie, 2012.
[33] A. Kibboua, M.N. Farsi, J.L. Chatelain, B. Guillier, H. Bechtoula, Y. Mehani, Modal analysis and ambient vibration measurements on mila-algeria cable stayed bridge, Struct. Eng. Mech. 29 (2) (2008) 171–186.

[34] F. Rojas, J.C. Anderson, L.M. Massone, A nonlinear quadrilateral thin flat layered shell element for the modelling of reinforced concrete wall structures, Bull. Earthq. Eng. 17 (12) (2019) 6491.
[35] R.D. Cook, Concepts and Applications of Finite Element. Analysis, John Wiley, New York, NY, 1989.
[36] F. Dashti, R.P. Dhakal, S. Pampanin, A parametric investigation on applicability of the curved shell finite element model to nonlinear response prediction of planar RC walls, Bull. Earthq. Eng. (2019).
[37] Naze, P.A., Contribution to the damage measurement of reinforced concrete buildings under seismic solicitations: proposal of an improvement for the evaluation of the damaging potential of a signal and of the damage for the girders structures: introduction to the reliability analysis of the damage in terms of the damaging potential of a seismic signal.Institut National des Sciences Appliquées (INSA), 69 - Villeurbanne (France).
[38] A.J.M. Ferreira, Design of a Sofa for a Passenger Train, Faculdad de Engenharia da Universidade do Porto, Portugal, Composite Structures 4. Science, Elsevier Appl, 1987.
[39] Ferdjani O., Behaviour of a One Cell Prestressed Concrete Box Girder Bridge-Analytical Study, Master of Engineering Thesis, Department of Civil Engineering and Applied Mechanics, McGill University, Montreal, Canada, March 1987.
[40] Biryukovich K.L., Biryukovich Yu L., Biryukovich D.L., Glass-fiber-reinforced cement. Kiev: Budivelnik; 1964 [CERA Translation, 1965, No. 12].
[41] A.J. Majumdar, J.R. Ryder, Glass fiber reinforcement of cement products, Glass Technol. 9 (3) (1968) 78–84.
[42] J.P. Romualdi, G.B. Batson, Mechanics of crack arrest in concrete, J. Eng. Mech. Div. ASCE Proc. 89 (EM3) (1963), 147–68.
[43] Romualdi J.P., Mandel J.A., Tensile strength of concrete affected by uniformly distributed and closely spaced short lengths of wire reinforcement, Journal ACI 1964:657–70.
[44] M. Andrzej, Brandt, Fiber reinforced cement-based (FRC) composites after over 40 years of development in building and civil engineering, Compos. Struct. 86 (1–3) (2008).
[45] Soufeiania Leila, Sudharshan N.Ramanb, Mohd Zamin BinJumaata, Ubagaram JohnsonAlengarama, GhasemGhadyania, PriyanMendisc, Influences of the volume fraction and shape of steel fibers on fiber-reinforced concrete subjected to dynamic loading, A review, Eng. Struct. 124 (2016).
[46] Doo-Yeol Yoo, Soonho Kim, Gi-Joon Park, Jung-Jun Park, Sung-Wook Kim, Effects of fiber shape, aspect ratio, and volume fraction on flexural behavior of ultra-high-performance fiber-reinforced cement composites, Compos. Struct. 174 (2017).
[47] Bathias, C., 2009, Matériaux Composites, ed. Dunod.
[48] C.G.S ,2003, RPA: Règles parasismiques algériennes, RPA99/version 2003.